Int J Appl Earth Obs Geoinformation 93 (2020) 102216

Contents lists available at ScienceDirect

Int J Appl Earth Obs Geoinformation

journal homepage: www.elsevier.com/locate/jag

Use of Sentinel-2 MSI data to monitor crop irrigation in Mediterranean areas

F. Maselli[a,*], P. Battista[a], M. Chiesi[a], B. Rapi[a], L. Angeli[b], L. Fibbi[a], R. Magno[a], B. Gozzini[a,b]

[a] IBE-CNR, Via Madonna del Piano, 10, 50019, Sesto Fiorentino, FI, Italy
[b] LaMMA Consortium, Via Madonna del Piano, 10, 50019, Sesto Fiorentino, FI, Italy

ARTICLE INFO

Keywords:
Annual crops
Actual evapotranspiration
Irrigation
NDVI

ABSTRACT

The availability of accurate information on the water consumed for crop irrigation is of vital importance to support compatible and sustainable environmental policies in arid and semi-arid regions. This has promoted several studies about the use of remote sensing data to monitor irrigated croplands, which are mostly based on statistical classification and/or regression techniques. The current paper proposes a new semi-empirical approach that relies on a water balance logic and does not require local tuning. The method stems from recent investigations which demonstrated the possibility of combining standard meteorological data and Sentinel-2 (S-2) Multi Spectral Instrument (MSI) NDVI images to estimate the actual evapotranspiration (ETa) of irrigated Mediterranean croplands. This ETa estimation method is adapted to drive a simplified site water balance which, for each 10-m S-2 MSI pixel, predicts the irrigation water (IW), i.e. the water which is consumed in addition to that naturally supplied by rainfall. The new method, fed with ground and satellite data from two years (2018–2019), is tested in a Mediterranean area around the town of Grosseto (Central Italy), that is covered by a particularly complex mosaic of rainfed and irrigated crops. The results obtained are first assessed qualitatively for some fields grown with known winter, spring and summer crops. Next, the IW estimates are evaluated quantitatively versus ground measurements taken over two irrigated fields, the first grown with processing tomato in 2018 and the second with early corn in 2019. Finally, the IW estimates are statistically analyzed against various datasets informative on local agricultural practices in the two years. All these analyses indicate that the proposed method is capable of predicting both the intensity and timing of the IW supply in the study area. The method, in fact, correctly identifies rainfed and irrigated crops and, in the latter case, accurately predicts the IW actually supplied. The results of the quantitative tests performed on tomato and corn show that over 50 % and 70 % of the measured IW variance is explained on daily and weekly bases, respectively, with corresponding mean bias errors below 0.3 mm/day and 2.0 mm/week. Similar indications are produced by the qualitative tests; reasonable IW estimates are obtained for all winter, springs and summer crops grown in the study area during 2018 and 2019.

1. Introduction

Water is a major environmental resource whose availability is increasingly limited in arid and semi-arid areas due to both the rising requirements for human activities and the effects of climate change (Famiglietti and Rodell, 2013; Jalilvand et al., 2019). This is particularly the case in Mediterranean regions, where there is a contemporaneous increase in water needs for several competing uses (civil, agricultural, industrial) and a decrease of water availability because of negative rainfall trends (Giorgi et al., 2004; Hartmann et al., 2013). The assessment of actual water uses is therefore becoming of primary importance for public authorities in most Mediterranean areas, such as Central and Southern Italy.

In these regions agricultural activities are the main consumer of water resources, mainly due to irrigation requirements for extensive summer croplands (corn, tomato, sunflower, etc.). Because of the great variety of agricultural practices applied to these crops, such requirements are extremely variable both in space and in time (Guzinski and Nieto, 2019). Consequently, estimating crop irrigation on wide land areas is a non trivial issue, for which conventional, ground based methods can provide only a partial solution. Such methods, in fact, are labor and time intensive, and are therefore usually applied only for assessing crop irrigation over relatively small land areas and brief time periods (Giannini and Bagnoni, 2000).

Remote sensing techniques offer an alternative, cost-effective opportunity to obtain information related to crop water consume (e.g.

* Corresponding author.
E-mail address: fabio.maselli@cnr.it (F. Maselli).

https://doi.org/10.1016/j.jag.2020.102216
Received 16 March 2020; Received in revised form 29 July 2020; Accepted 5 August 2020

crop type, extent and condition) on various spatial and temporal scales. In particular, optical and thermal datasets have been widely utilized to estimate the distribution of irrigated crops in different regions of the globe (Ozdogan et al., 2010; Ambika et al., 2016; Zhang et al., 2016). Ozdogan and Gutman (2008), for example, applied a four-step procedure to ancillary and MODIS data to map irrigated areas at continental level in the USA; these authors used nonparametric classification and regression algorithms in order to address the complex spatio-temporal patterns of irrigated lands. Peña-Arancibia et al. (2014) utilized a nonparametric statistical approach based on ground and satellite products (both at medium and high spatial resolution) to identify summer cropped irrigated areas in Australia; the nonparametric Random Forest model was trained with local data and then applied to obtain a regional-scale identification of irrigated crops. The same classifier preceded by the segmentation of Spot 6 imagery was successfully applied by Vogels et al. (2019), to map irrigated agriculture in the Central Rift Valley, Ethiopia. A similar approach based on fused MODIS and Landsat datasets was applied by Chen et al. (2018); these authors, however, detected water supplement events by means of a threshold-based model which is hardly applicable in different environmental conditions.

In general, statistical approaches have obtained promising results, but present relevant shortcomings due to the need for proper training over representative ground samples and to the usually limited generalization capacity. A different, more deterministic strategy could therefore be based on the identification of water deficit conditions which are presumably associated to irrigation, i.e. of cases where crop actual evapotranspiration (ETa) significantly exceeds water availability from natural sources. This strategy implicitly assumes that the water used for irrigation approximately corresponds to the not-rain water consumed by crops (Steduto et al., 2012). This assumption can be considered to be reasonable in all cases when the cost of extracting and distributing irrigation water (IW) discourages misuses of this resource, as is common in many Mediterranean regions.

The application of this strategy requires the daily estimation of both rainfall and crop ETa over wide land areas. The production of rainfall maps from ground measurements is by now a consolidated practice (e.g. Thornton et al., 1997; Mair and Fares, 2011), while the prediction of ETa can be performed through remote sensing techniques based on two approaches, i.e. the energy balance and the water balance (e.g. Glenn et al., 2007; Pereira et al., 2015). Both approaches have advantages and limitations, but energy balance methods are problematic to apply operationally in areas with complex irrigation patterns due to the insufficient spatio-temporal resolutions of existing satellite thermal imagery (Calera et al., 2017). Most operational applications are therefore performed through water balance methods, which usually rely on the same principle of the classical FAO crop coefficient (Kc) strategy (Allen et al., 1998). This strategy combines estimates of potential or reference evapotranspiration (ET_0) with multitemporal Kc derived from remotely sensed vegetation indices, among which the normalized difference vegetation index (NDVI) is the most popular and commonly used (Senay, 2008; Glenn et al., 2010).

The original Kc-NDVI approach does not account for the impact of water stress and is therefore applicable only to well-watered crops, while overestimates ETa in the other cases (Gonzalez-Dugo et al., 2009). A similar issue partially affects the evapotranspiration products routinely obtained at several spatial and temporal resolutions by the MOD16 algorithm, which is based on the well-known Penman-Monteith (P-M) equation (Mu et al., 2011; He et al., 2019). These problems are fundamentally due the non consideration of soil water shortage, which exerts the most immediate and effective limitation on ETa. This issue was addressed by Maselli et al. (2014), who proposed a method capable of predicting ETa in water limited Mediterranean environments. That method, named NDVI-Cws, accounts for the short-term effect of soil water shortage by a scalar derived from standard meteorological data, and is therefore intrinsically suitable for rainfed ecosystems.

The operational application of this and similar methods can obviously benefit from the recent availability of Sentinel-2 (S-2) Multi Spectral Instrument (MSI) images, which have high spatial resolution (10 m) and frequent revisiting time (around 3–4 days at our latitudes) (Drusch et al., 2012). The use of these images allows the clear identification of most cropped fields, and consequently the accurate estimation of relevant NDVI evolutions (Belgiu and Csillik, 2018; Maselli et al., 2020a). This has supported an improvement of the NDVI-Cws method which addresses the cases where water additional to rainfall can be provided to summer crops, which usually correspond to irrigated conditions (Maselli et al., 2020b). As fully explained in the same article, the methodological improvement was obtained by modifying the water stress scalar based on the crop NDVI evolution during the dry season.

The combination of conventional meteorological data and S-2 MSI images is therefore potentially suited to produce information for identifying and characterizing irrigated fields. This subject has been recently explored by Vanino et al. (2018), who investigated the use of albedo and leaf area index estimates obtained from S-2 images to characterize a tomato field in Central Italy. In particular, their study concerned the incorporation of the S-2 estimates in a P-M approach for assessing crop evapotranspiration and water requirement in standard conditions. This method is therefore suited to predict the maximum water requirement of irrigated crops having known spatio-temporal distribution; conversely, it is not appropriate to identify and quantify actual crop irrigation in areas where such distribution is complex, irregular and anyway unknown.

The current paper postulates that this objective can be pursued by a proper application of the modified NDVI-Cws method (Maselli et al., 2020b). This possibility is investigated concerning an agricultural plain around the town of Grosseto (Central Italy), where fields of variable size are grown with rainfed winter and spring crops (wheat, barley, alfalfa, sorghum, etc.) intermingled with irrigated summer crops (corn, tomato, sunflower, vegetables, etc.). Most of these crops show diversified growing cycles depending on the application of different agricultural practices, which increases the environmental heterogeneity of the study area and, consequently, the difficulty of identifying and characterizing irrigated fields. The experiment has concerned two growing seasons, 2018 and 2019, during which the availability of data from both twin S-2 satellites has allowed a full characterization of crop NDVI evolutions.

The paper is organized as follows. First, the IW prediction method is fully illustrated, including the parts presented in previous publications and the innovation currently developed for completing the prediction of crop irrigation. The study area and data are then described, followed by the data processing and results. The two final sections present a discussion of the experimental findings obtained and the conclusions on their implications and consequences.

2. IW prediction method

The methodology developed for identifying and characterizing crop irrigation stems from previous studies dealing with ETa estimation in Mediterranean areas and is completed relying on a conceptual framework derived from the knowledge of local agricultural practices. In particular, an assumption is used which is valid in the study area and, more generally, in all cases when water resources are limited and anyway expensive. In these situations, farmers tend to estimate the water which is consumed by the crop during each stage of the growing cycle and consequently regulate irrigation supply. This implies that the IW actually used roughly corresponds to the water needed by plants minus the contribution of the rainfalls occurred.

The methodology can be applied on a daily basis at different spatial scales (from single pixel to field or plot) and is divided into two sequential steps. The first, already presented in previous publications, identifies vegetated areas where water supply additional to rainfall can be presumed and predicts the respective actual transpiration (Tr_A). The non consideration of evaporation is due to the prevalent form of irrigation which is used in the study area, i.e. drip irrigation, which

concentrates water on vegetated surfaces and minimizes the loss from bare soil. The supposed irrigation requirement is then predicted in a second, innovative step, which is based on a simplified site water balance taking into account both most recent rainfalls and the rain water stored in the soil. These two steps are described in the following subsections.

2.1. Estimation of Tr_A for irrigated crops

This step is based on an operational method, NDVI-Cws, which was proposed to estimate daily ETa in water limited Mediterranean ecosystems through the combination of ground meteorological data and remotely sensed NDVI imagery (Maselli et al., 2014). This method uses the fractional vegetation cover to account for the contribution of site transpiration and evaporation; the actual crop evapotranspiration of day i (ETa_i) can therefore be predicted as the sum of the two terms:

$$ETa_i = ET_{0i} \cdot 1.2 \cdot FVC_i \cdot (0.5 + 0.5 \cdot AW_i) + ET_{0i} \cdot 0.2 \cdot (1 - FVC_i) \cdot AW_i \quad (1)$$

where ET_0 is potential evapotranspiration, FVC is the fractional vegetation cover and AW is a short term water stress scalar, all referred to day i; 1.2 and 0.2 correspond to the maximum crop coefficient for herbaceous vegetation and soil, respectively.

FVC is linearly derived from NDVI (Gutman and Ignatov, 1998) while the water stress scalar is computed as:

$$AW_i = \frac{\sum_i^{i-29} Prec_i}{\sum_i^{i-29} ETo_i} \quad (2)$$

where the summation of precipitation (Prec) is bounded by that of ET_0, so that the scalar can range from 0 (full meteorological water stress) to 1 (no stress). Being the water stress scalar computed from the observed precipitation, the NDVI-Cws method is suitable for rainfed ecosystems, while it must be adapted in cases when water is supplied additional to rainfall (Maselli et al., 2014). The modification put forward by Maselli et al. (2020b) addresses these cases, which, for summer crops, usually corresponds to irrigated conditions. The same publication reports a full description of the modified algorithm and its implications, which are summarized in the following paragraphs.

The modification deactivates the water stress scalar (i.e. increases it up to 1) when a divergence is detected in the temporal evolutions of meteorological water stress and NDVI (or FVC). In particular, a full or partial deactivation is performed when FVC is increasing or close to the seasonal maximum during the summer water stress period. Mathematically, the modified water stress scalar of day i, AW_{FVCi}, is obtained by keeping the maximum of the original AW_i and of a normalized FVC_i, (FVC_{NORMi}), computed as:

$$FVC_{NORMi} = \frac{(FVCi - FVCmin)}{(FVCmax - FVCmin)} \quad (3)$$

where FVCmin and FVCmax are found progressively since the start of the dry season (i.e. when AW_i becomes lower than 1).

Consequently, the transpiration of irrigated crops for day i, Ta_i can be predicted as:

$$Ta_i = ET_{0i} \cdot 1.2 \cdot FVC_i \cdot (0.5 + 0.5 \cdot AW_{FVCi}) \quad (4)$$

As can be easily understood, Ta corresponds to the transpiration of a rainfed crop when the NDVI approaches the progressive minimum during the dry season (i.e. $AW_{FVC} = AW$), while it corresponds to the transpiration of a fully or partially irrigated crop when the NDVI is equal or close to the dry season maximum, respectively (i.e. $AW_{FVC} > AW$). Thus, the algorithm is more sensitive to NDVI variations during the dry season than to absolute NDVI values. This accounts for both the diversified NDVI values at the beginning of the water stress period and the variable NDVI responses to the seasonal meteorological evolution. In all cases, however, the NDVI of annual grasses and crops is expected to increase or be close to the dry period maximum only if water is supplied additional to rainfall.

The algorithm therefore combines indicators of meteorological water stress and temporal NDVI variation for the dynamic identification of a disequilibrium between water supplied by rainfall and required by the plants, which can provide the basis for the subsequent prediction of crop irrigation.

2.2. Estimation of irrigation water

The daily water requirement of irrigated crops is assumed to be estimable from the actual transpiration averaged over a short time period, i.e. the current and the previous two days. In order to predict the actual IW, however, this amount must be reduced by the rainfall which may be fallen in the same period or is accumulated in the soil during the previous weeks.

Such correction is therefore performed in two phases. First, the predicted IW is set to 0 when the effective rainfall (i.e. rain minus ET_0) of the last three days is positive, based on the obvious consideration that no irrigation is applied during rainy periods. Second, the contribution of less recent rainfalls to soil water storage is estimated using the logical framework exposed in Maselli et al. (2020b), i.e. assuming that AW_{FVC} and AW are proportional to the total and the rain water transpired by the crop, respectively. Thus, the normalized difference between the two terms can be taken as indicative of the water amount presumably provided by irrigation and can be used to correct transpired water. Based on this reasoning, irrigation water for non-rainy day i (IW_i) can be predicted as:

$$IW_i = \frac{\sum_i^{i-2} Ta_i}{3} \bullet \frac{(AW_{FVCi} - AW_i)}{AW_{FVCi}} \quad (5)$$

The IW computed by this algorithm tends to recent crop Ta when $AW_{FVC} > AW$ and AW approaches 0, while it tends to 0 just after a rainfall or when AW_{FVC} coincides with AW. The latter case occurs when AW is 1, which implies that precipitation exceeds ET_0 in the last month, or when FVC_{NORM} is lower than AW, which implies that the crop NDVI is close to the dry season minimum due to the effect of water stress or senescence.

3. Study area and data

3.1. Study area

The study area has a size of 20 × 20 km^2 and is situated in Southern Tuscany (Italy, 42.70–42.89 °N, 10.95–11.20 °E, Fig. 1). The climate of this plain is Mediterranean sub-arid, with hot, dry summers and mild, relatively wet winters. The mean annual temperature is 15.9 °C and the annual rainfall is about 650 mm, concentrated in fall and spring. The area is mostly covered by agricultural fields interspersed with forest, rural and urban lands; winter (e.g. wheat, barley), spring (e.g. alfalfa, chickpea) and summer (e.g. sunflower, tomato, corn) crops are all widely grown. Winter crops are always rainfed, while supplemental irrigation is provided to many spring crops depending on seasonal meteorology; summer crops are usually irrigated during the dry season.

Some fields cultivated with the crops most widespread in the area during the 2018 and 2019 growing seasons were selected for illustrating the general functioning of the IW estimation method described. Additionally, the study focused on two experimental fields grown with the most important irrigated summer crops, i.e. tomato and corn, in 2018 and 2019, respectively.

The first field has a size of about 350 × 300 m^2 and in 2018 was grown with processing tomato (*Solanum lycopersicum* L.). Small tomato plants (H1015 e Delfo F1 varieties) were transplanted at the end of April (28th April) and fruits were picked at the end of July (31st July); drip irrigation was applied from mid-June to crop harvesting. The corn

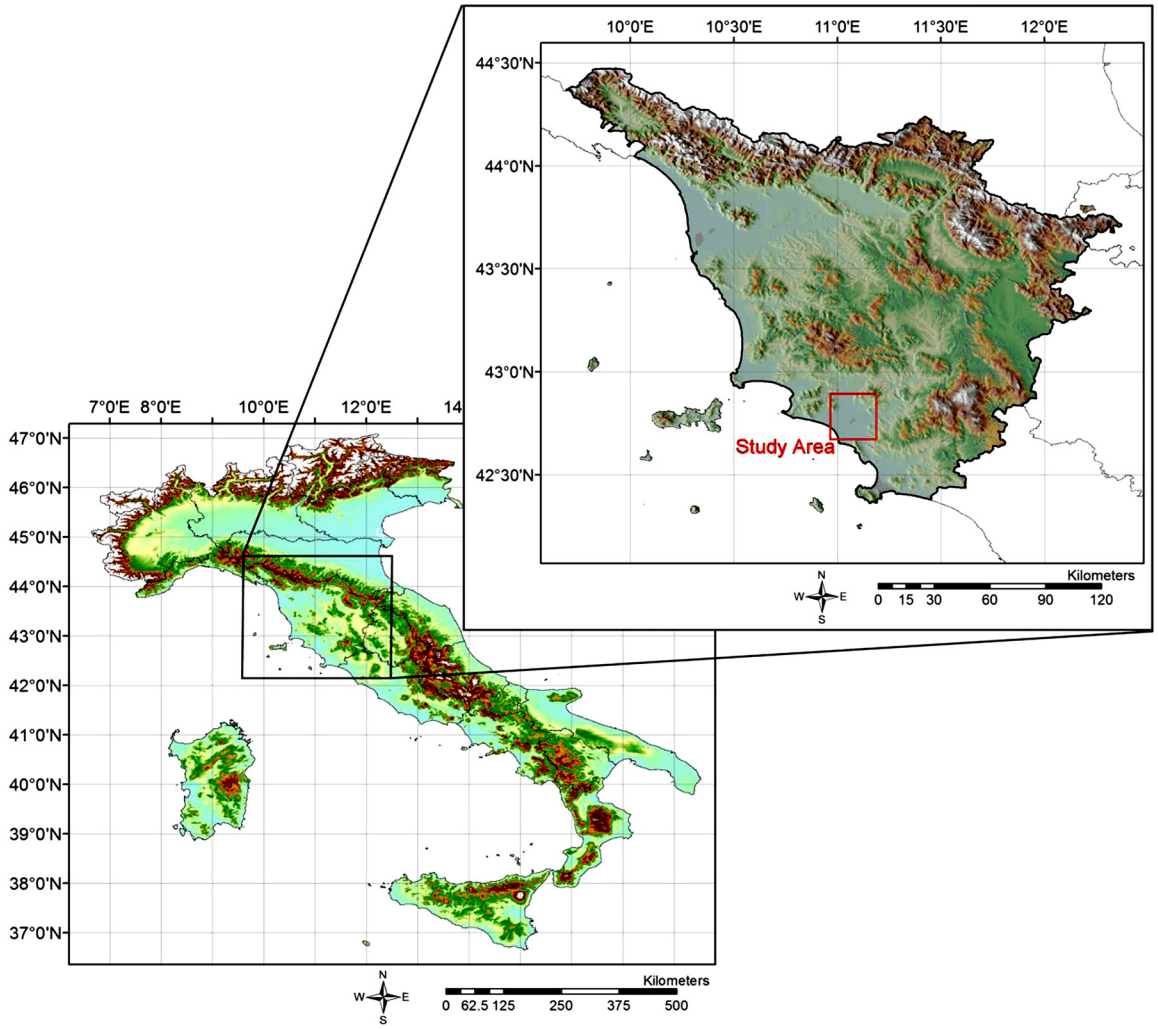

Fig. 1. Digital elevation model of Italy showing the geographical position of Tuscany (bottom left box), and, enlarged, the same region with the location of the study area (upper right box).

(*Zea mays* L.) field is close to the former and has a size of 600 × 450 m^2; it was sowed in the second half of April (18th April) and harvested on 20 August 2019; drip irrigation was applied from 12nd June to crop harvesting. In both cases, the water used for irrigation (IW) was extracted from deep wells (20 − 30 m) and provided to the crops following a schedule decided by the farmers on the basis of their practical experience.

3.2. Study data

Information on the crop type, agricultural practices and crop calendars used in some fields during 2018 was obtained from personal contacts with local farmers (Table 1).

Table 1
Main features of the exemplary rainfed and irrigated cropped fields selected for describing the model functioning in the 2018 growing season (Figs. 5 and 6).

Crop type	Sowing	Transplanting	Harvesting	Irrigation
Set-aside	–	–	–	No
Winter wheat	November (2017)		Mid-June	No
Chickpea	February		Early July	No
Late tomato		Late May	Early September	Yes
Early corn	Mid-April		Late August	Yes
Late corn	Mid-June		Mid-October	Yes

The two experimental fields were instead continuously monitored during the respective crop growing cycles through a fully equipped station collecting standard agrometeorological measurements (i.e. daily minimum and maximum air temperature, precipitation, solar radiation and wind speed and direction) and a water meter measuring daily IW. Additionally, phenological observations were taken for both the tomato field in 2018 and the corn field in 2019.

Interpolated meteorological data were derived for the two study years from a regional database which provides daily air temperature and precipitation at 250-m spatial resolution; the interpolation was based on about 100 weather stations for temperature and 160 for precipitation. These data were checked for consistency against those collected by the ground stations at the tomato and corn fields during the respective growing seasons.

A 1:10000 scale map describing the area covered by annual crops was obtained from the same regional database. This map was not informative on the crop types actually grown during the two study years; for part of the investigated area (30–40 % of that covered by annual crops) this information was derived from the regional ARTEA database of cultivated fields (http://dati.toscana.it/dataset/artea-piani-colturali-grafici-annualita-2019).

Imagery taken by the twin S-2 A and B satellites by means of the MSI sensor was used for both 2018 and 2019. All available S-2 MSI images of these two years covering the study area were downloaded in an ortho-rectified, pre-processed L-2A format from the ESA website

(https://sentinel.esa.int/web/sentinel/sentinel-data-access).

4. Data processing

The same data processing chain was applied for both study years, consisting of the following main steps.

4.1. Preprocessing of meteorological data

Daily solar radiation was estimated from the interpolated temperature and rainfall through the MT-Clim algorithm (Thornton et al., 2000). Next, daily ET_0 was computed from temperature and solar radiation by the algorithm of Jensen and Heise (1963), and was combined with precipitation to predict the meteorological water stress scalar AW.

4.2. Preprocessing of S-2 MSI NDVI images

10-m spatial resolution NDVI images were computed from the available S-2 MSI dataset and subjected to a maximum value composite (MVC) operation over half-month periods. A further temporal filtering was applied to the MVC images in order to reduce residual atmospheric disturbances (see Maselli et al., 2014, for details). NDVI was then converted into FVC and interpolated on a daily basis as fully described in the same paper.

4.3. Prediction of IW

The daily Ta of all annual crops in the study area was predicted at S-2 MSI pixel resolution by combining the interpolated meteorological and FVC data through Eqs. (3) and (4). Eq. (5) was then applied to predict IW with the same spatial and temporal resolutions. The entire operation was performed only for the seasons during which irrigation can be supposed to be active, i.e. from mid-May to mid-October 2018 and 2019.

4.4. Evaluation of IW estimates

The predicted IW was assessed through: i) a qualitative evaluation conducted on the exemplary fields grown with known rainfed and irrigated crops in 2018; ii) a quantitative assessment performed through comparison with the daily ground measurements taken in the two experimental fields (tomato in 2018 and corn in 2019), summarizing the results by means of common accuracy statistics (r^2, RMSE and MBE); iii) a statistical analysis of the agro-meteorological information available about several other fields grown with known crops in the two study years.

5. Results

5.1. Meteorological, NDVI and IW patterns in 2018 and 2019

The diagrams of Fig. 2A-B summarize the meteorology of the study area in 2018 and 2019. Spring rainfalls are relatively abundant till mid-June in 2018 and slightly earlier in 2019. Summer rainfalls are similarly low in the two years (80 − 100 mm), while ET_0 is lower in 2018 than in 2019 (around 530 versus 560 mm, respectively); the ET_0 difference between the two years is mainly due to an extremely hot period from mid-June to mid-July 2019. These weather patterns induce a clear water stress period from June to September, but the start of the dry season is around mid-June in 2018 and at the beginning of the same month in 2019.

Two MSI NDVI MVC images corresponding to the peak of the dry period (second half of July) in the two years are shown in Fig. 3A-B. These images clearly display the fragmented nature of the agricultural area, where a variety of crops with different phenological cycles are intermingled. Most cropped fields show low NDVI values, which indicates their rainfed condition; conversely, the few cropped fields with high NDVI can be presumed to be irrigated.

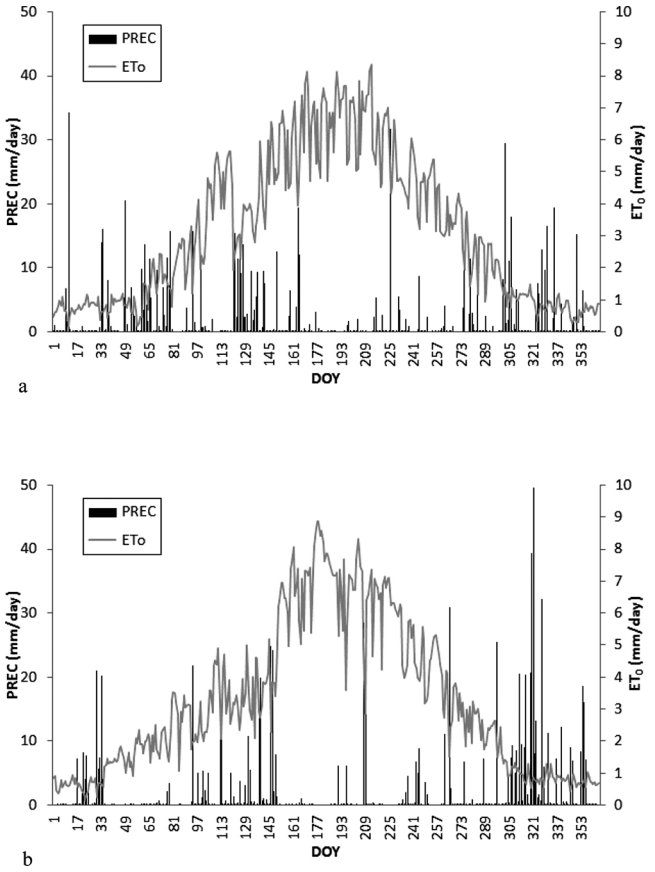

Fig. 2. Annual time series of precipitation (PREC) and potential evapotranspiration (ET0) during 2018 (A) and 2019 (B).

This hypothesis is confirmed by the maps of total IW obtained by the described procedure for 2018 and 2019, that are shown in Fig. 4A-B. Most areas, which are likely covered by winter crops or semi-natural meadows, have very low or null estimated IW (below 25 mm). Relatively high levels of IW are instead predicted for a few fields of various size, mostly ranging from 100 to about 400 mm.

The inter-comparison between the IW maps of the two years indicates a greater spread and intensity of irrigation in 2019. The total IW predicted over the study area equals 10,128,594 m^3 in 2018 and 12,697,793 m^3 in 2019, which corresponds to a relative increase of 25 %. About half of this difference can be attributed to the different meteorological evolutions of the two years. As previously noted, in fact, in 2019 ET_0 was higher and spring rainfall stopped earlier than in 2018; the difference between ET_0 and precipitation (i.e. the water deficit) in the months June-August equals 457 mm in 2018 and 514 mm in 2019, corresponding to a relative increase of 12.5 %. This different meteorology presumably led to more stressed conditions for summer crops and to a consequent pressure to increase irrigation in 2019. This adds to the presumably increased extent of irrigated areas in 2019, which is in agreement with the agricultural statistics reported in the aforementioned regional database of ARTEA. Even though, as previously noted, such statistics do not cover all cropped fields, they indicate that in the province of Grosseto the area grown with irrigated tomato and corn increased by more than 50 % from 2018 to 2019.

5.2. Examples of estimated NDVI, Ta and IW evolutions

Fig. 5A–C shows some typical NDVI evolutions of rainfed annual crops in 2018, together with the respective estimates of Ta and IW;

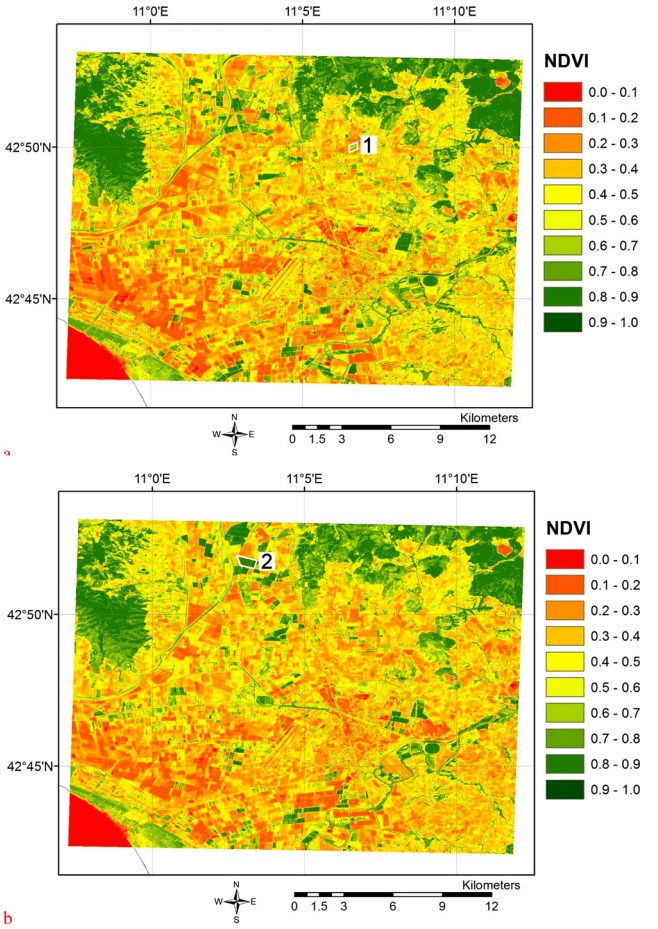

Fig. 3. Examples of Sentinel-2 MVC NDVI images of the second half of July 2018 (A) and 2019 (B); the position of the experimental tomato and corn fields is indicated by 1 and 2 in the respective images.

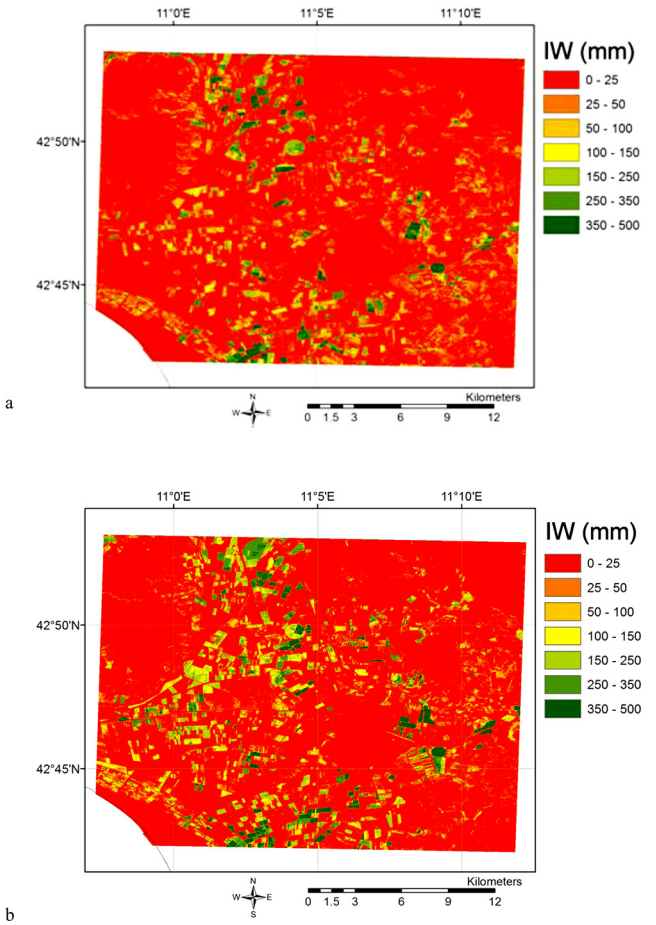

Fig. 4. Maps of total IW predicted by the described procedure for 2018 (A) and 2019 (B).

information on the type and main features of these crops is provided in Table 1. The first case, which corresponds to set-aside management, shows moderate NDVI and Ta variations, with a primary peak at the end of April followed by a slow decrease in the dry summer period and a slight recovery in autumn. The NDVI decrease from spring to summer is typical of Mediterranean semi-natural grasslands and leads to a nearly null IW estimate. Wheat, which is the main winter crop in the area, has a clearer NDVI peak at the end of April, followed by a rapid drop; as a consequence of this trend, Ta is high until May, but IW is nearly null for the whole growing season. The case is similar for chickpea, a drought resistant spring crop which is only occasionally irrigated. This crop shows a later growing cycle and an NDVI peak in May, followed by a drop after the start of the dry season which still produces an almost null IW estimate.

The three NDVI evolutions of Fig. 6A–C are representative of two summer crops, tomato and corn, which are grown in irrigated condition (see Table 1). The first crop corresponds to a late variety of tomato, that is transplanted in May and reaches an NDVI maximum in August, before harvesting at the beginning of September. Tomato Ta follows a similar pattern which mostly corresponds to IW; the latter, however, is lower than Ta at the beginning and end of the growing cycle, when rainfall contributes to soil water recharge and, consequently, crop transpiration (see Fig. 2A). Total IW is estimated around 290 mm. The second crop, early corn, is planted in April, reaches an NDVI maximum at the end of June, followed by a long plateau before harvesting at the end of August. Corn Ta and IW follow this temporal evolution with the same patterns observed above, i.e. reduced IW at the beginning and end of the growing cycle due to rainfall. The longer growing cycle with respect to tomato yields a higher IW estimated total (400 mm). The second corn variety, late, is preceded by a spring crop (ryegrass), that is grown in rainfed condition. Corn is planted in June, reaches a maximum in August and is harvested at the beginning of October. Accordingly, NDVI and Ta show two peaks, the first, of ryegrass, in April and the second, of corn, in late July-beginning of August. The first NDVI peak precedes the start of the dry season and is followed by a decrease which inhibits the estimation of IW; only the second NDVI is therefore correctly identified as corresponding to irrigated condition. Again, estimated IW is lower than Ta after mid-August, when part of soil water is provided by rainfall, and reaches a seasonal total of about 330 mm.

The NDVI, Ta and IW evolutions found in 2019 for winter, spring and summer crops are similar to those of 2018, with only slight differences in intensity and timing due to the different meteorology of the year and the consequent agricultural calendar; these evolutions are therefore not currently shown.

5.3. Validation of estimated IW in the two experimental fields

Table 2 reports the ground information for the two experimental fields, whose geographical position is shown in Fig. 3A-B. The NDVI evolution of the tomato field in 2018 is shown in Fig. 7. This is typical for a summer crop planted in April, fully irrigated from mid-June and harvested at the end of July. The same figure shows the daily irrigation really applied to the field, which can be compared to the respective estimated IW. When evaluating these results, however, it must be kept in mind that the exact irrigation days cannot be predicted, since they are partly due to random events (i.e. technical and practical issues related to water extraction and distribution). This obviously decreases the

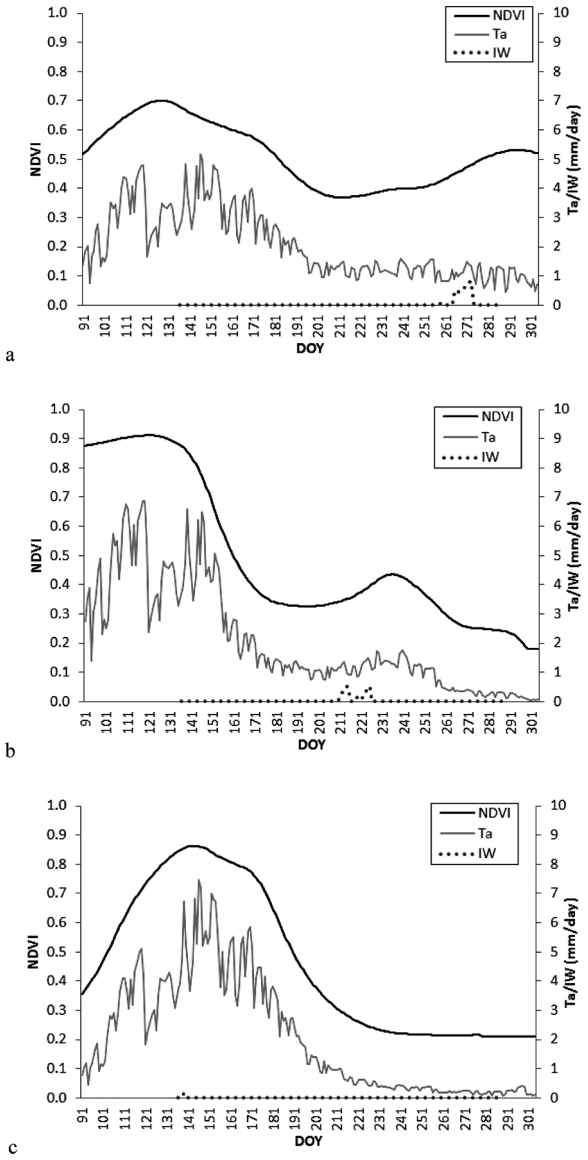

Fig. 5. Seasonal evolutions of NDVI, Ta and IW predicted for some typical rainfed crops in 2018: semi-natural grassland (A), winter wheat (B) and chickpea (C).

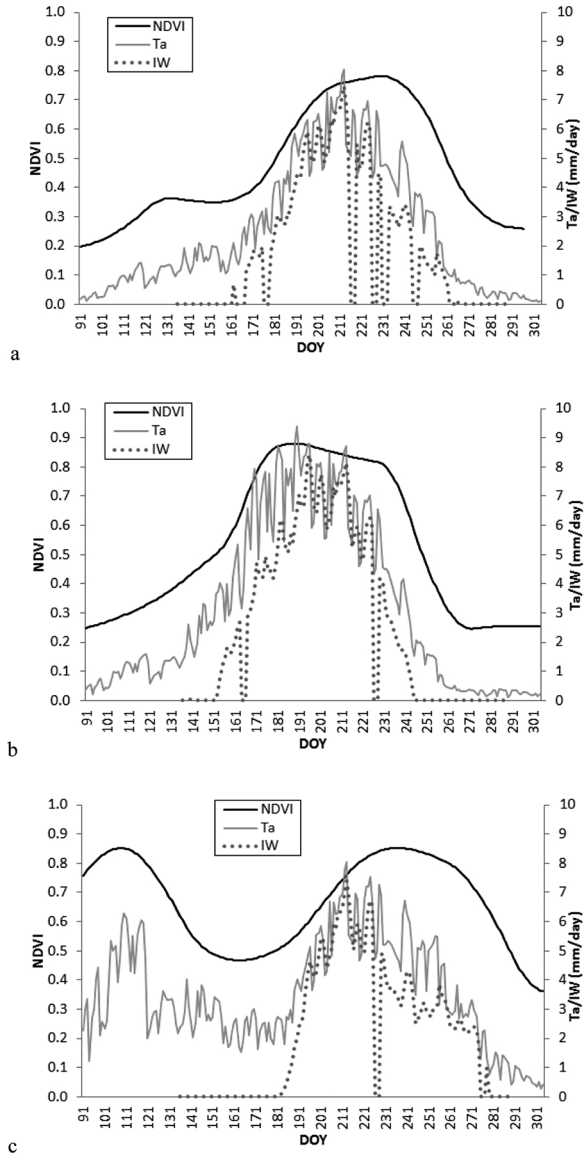

Fig. 6. Seasonal evolutions of NDVI, Ta and IW predicted for some typical irrigated crops in 2018: late tomato (A), early corn (B) and late corn (C).

agreement between daily IW measurements and estimates, affecting in particular the observed r^2 and RMSE. MBE is instead less influenced by this issue, and is actually very low (-0.13 mm/day), indicating that the total amount of estimated IW is close to the respective measurement (202 versus 222 mm). The good accuracy of the estimates is confirmed by aggregating the data on a weekly basis, which obviously mitigates the aforementioned problem due to the exact identification of irrigation days; this operation notably increases the determination coefficient and reduces the RMSE in relative terms (i.e. referred to the same time period).

The same general trend can be observed in Fig. 8, which shows the evolutions of NDVI and of measured and estimated IW for the experimental corn field in 2019. This crop was planted in mid- April, irrigated after mid-June and harvested after mid-August (Table 2). Consequently, the total water amount provided by irrigation is higher than for tomato (around 300 mm), and is slightly overestimated by the described method (338 mm), mostly due to an IW overestimation around the end of the corn growing cycle (late August). This corresponds to a low MBE (0.24 mm/day), while the other two accuracy statistics are still only moderate, being affected by the above mentioned problem in identifying irrigation days. Such problem is still mitigated by aggregating the data on a weekly basis, which significantly improves the accordance between measurements and estimates.

Overall, the accuracy obtained in the two case studies can be considered satisfactory, indicating the capacity of the applied procedure to simulate both intensity and timing of the irrigation events applied to the tomato and corn fields.

Table 2
Main features of the experimental tomato and corn fields used for assessing the model functioning in the 2018 and 2019 growing seasons, respectively (Figs. 7 and 8).

Crop type	Position	Sowing	Transplanting	Harvesting	Measured IW (mm)
Early tomato	42.833 °N, 11.111 °E		28/04/2018	31/07/2018	221
Early corn	42.862 °N, 11.050 °E	18/04/2019		19/08/2019	299

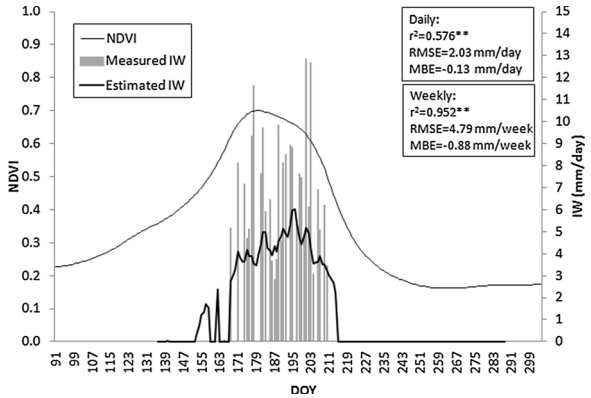

Fig. 7. Seasonal evolutions of NDVI and of measured and estimated IW obtained for the experimental tomato field in 2018; the accuracy statistics are computed on both daily and weekly time steps (** = highly significant correlation, P < 0.01).

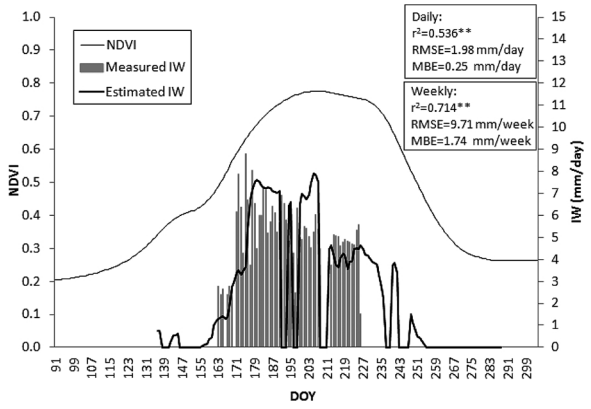

Fig. 8. Seasonal evolutions of NDVI and of measured and estimated IW obtained for the experimental corn field in 2019; the accuracy statistics are computed on both daily and weekly time steps (** = highly significant correlation, P < 0.01).

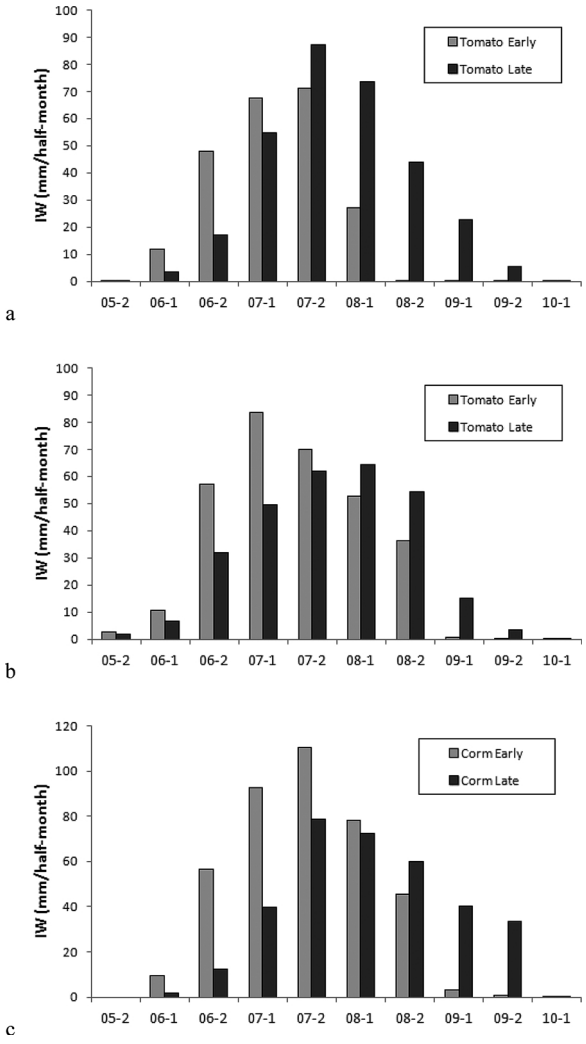

Fig. 9. Half-month period IW estimated for some fields grown with early and late varieties of tomato in 2018 and 2019 (A and B) and of corn in 2018 (C); the x axis indicate the half-month periods.

5.4. Analysis of estimated IW in other controlled fields

Table 3 reports the ground information obtained from personal contacts with local farmers for some fields grown with early and late varieties of tomato and corn in 2018 and of tomato in 2019. This information is useful to interpret Fig. 9A-C, which shows the mean IW estimated for these fields during all half-month periods of the two irrigation seasons (from 16th May to 15th October). In the first study year early tomato, which is transplanted in April, is irrigated from the beginning of the dry season (mid-June, Fig. 2A) to crop harvesting (beginning of August), with a peak in late July and a total of 226 mm. Late tomato, which is transplanted in June, is less irrigated at the beginning of the dry period, when plants are small, but irrigation lasts until early September, reaching a total of 308 mm. In 2019 early tomato, still transplanted in April, is irrigated from the beginning of the dry season (early June, Fig. 2B) to crop harvesting (mid-August); the longer and dryer growing season, joined to a higher ET_0 from mid-June to mid-July, produce an IW total much higher than in 2018 (314 mm). Late tomato, which is transplanted in May, is still less irrigated than the early variety at the beginning of the dry period, but irrigation lasts until September, for an IW slightly lower than that of 2018 (289 mm).

Both early and late corn varieties show IW totals higher than tomato in 2018, partly due to a longer growing cycle. The early variety, which is sowed in April, is irrigated already in June and has a high IW peak in July (200 mm), due to the co-occurrence of high NDVI (around 0.9) and ET_0 and nearly null rainfall (see Fig. 2A). Late corn, which is planted in June, is smaller and therefore less irrigated in July, but is irrigated also

Table 3
Main features of the tomato and corn fields characterized by personal contact with local farmers in the 2018 and 2019 growing seasons (Fig. 9A–C), with respective estimated IW.

Crop type	Year	N. fields	Sowing	Transplanting	Harvesting	Estimated IW (mm)
Early tomato	2018	3		End of April	Beginning of August	226
Late tomato	2018	6		Beginning of June	Beginning of September	308
Early tomato	2019	5		End of April	Mid-August	314
Late tomato	2019	5		End of May	Beginning of September	289
Early corn	2018	4	Mid-April		End of August	397
Late corn	2018	6	Mid-June		Beginning of October	339

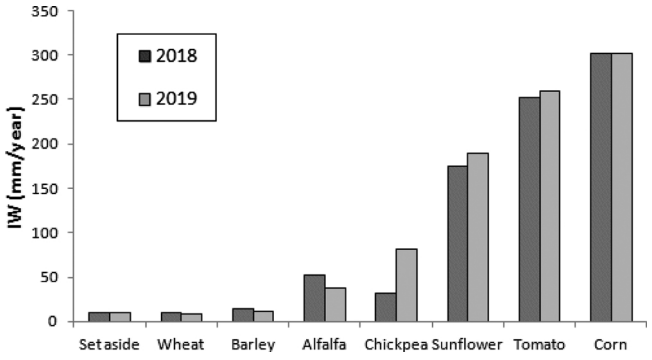

Fig. 10. Mean IW estimated for the main crop types grown in the study area in 2018 and 2019; the spatial distribution of these crops was taken from the regional database (see text for details).

in September, when ET_0 is lower. Consequent on these seasonal patterns, the IW total is higher for the early than for the late corn variety (397 versus 339 mm, respectively).

Overall, the estimated trends of IW are in accordance with the expected water requirements during the tomato and corn growing cycles; nearly all IW is predicted following the crop development stages and the seasonal meteorological evolutions, with only residual values after harvesting.

Fig. 10 shows the mean IW estimated for the eight main crop types reported by the regional ARTEA database, which are grown in more than 2000 fields covering over 8000 ha. In both study years the estimated IW approaches 0 for set-aside fields and for the two winter crops, wheat and barley, which are always grown in rainfed condition. Estimated IW is quite low (30 – 50 mm) for alfalfa and variable for chickpea (around 30 mm in 2018 and 80 mm in 2019). Both these crops are only occasionally watered, but are grown in different periods and under diversified agricultural practices. Alfalfa is a perennial species which is usually rainfed, with the exception of extremely dry periods when watering is supplied to avoid complete biomass loss. Chickpea is instead a spring crop to which, as mentioned previously, supplemental irrigation may be applied at the end of the growing cycle (end of June – beginning of July) depending on seasonal meteorology. This can explain the IW difference found in the two years, since June was relatively humid in 2018 and very hot and dry in 2019, determining different water requirements in the period preceding chickpea harvesting.

The different meteorological patterns of the two years can also explain the slightly higher IW predicted in 2019 for the three summer crops, which are variably irrigated. Estimated IW is intermediate for sunflower (about 180 mm), a drought resistant crop to which supplemental irrigation can be applied, and rises to around 250 and 300 mm for tomato and corn, respectively, which are always fully irrigated. These last IW averages are close to the IW measured in the experimental tomato and corn fields in 2018 and 2019 (around 220 and 300 mm, respectively). The same values are similar to the irrigation ranges suggested by local agricultural practices, which are around 50 – 100 mm for sunflower, 200 – 250 mm for tomato and 300 – 400 mm for corn (Giannini and Bagnoni, 2000).

6. Discussion

The methodology currently proposed relies on the basic assumption that the IW actually used approximately corresponds to the crop water requirements not satisfied by rainfall, which implies that local farmers are experienced and incentivized in the appropriate management of water resources. This assumption is realistic in the study area, where most farmers tend to irrigate parsimoniously due to the cost of drawing water from the most common sources, i.e. deep wells or distant artificial channels (see http://www.regione.toscana.it/censimentoagricoltura2010). Such expectation is supported by the current experimental findings, which consistently indicate that the IW utilized by local farmers is close to that actually required by the grown crops. Saving water is also the main reason for the local common use of drip irrigation, which justifies the current choice of considering Ta in place of ETa for IW prediction. This choice can be obviously changed when other, more water consuming irrigation systems (e.g. surface or sprinkler irrigation) are prevalently used in the examined area.

These considerations provide a plausible explanation for the disagreement of the current results with those obtained by Vanino et al. (2018), for a tomato field in an adjacent Italian region (Latium). These authors, in fact, found generalized over-irrigation and misuses of water resources, which can be likely ascribed to the prevalent, much cheaper water drawing from rivers and artificial channels in their study area. As noted in the introduction, another fundamental difference with respect to that study concerns the water quantity which is actually predicted. The method of Vanino et al. (2018), in fact, estimates the water requirements of crops in standard conditions, i.e. fully watered. Our method instead predicts the IW required for sustaining plants in the observed greenness conditions, which not necessarily correspond to full water satisfaction. This is due to both the possible incomplete FVC of the examined crops and the partial deactivation of the water stress scalar, which can limit the predicted T_A in the presence of not fully dense or green plants (Maselli et al., 2020b). Owing to all these reasons, our method provides a lower-limit estimate of IW, which can be exceeded unintentionally or intentionally in the common practice.

From a functional viewpoint, the method utilizes a previously proposed Ta estimation algorithm relying on the assumption that crop transpiration can be limited by both short- and long-term water stress, the first accounted for by a meteorological scalar and the latter by possible NDVI decrease (Maselli et al., 2014). Being the computation of the meteorological scalar originally based on rainfall estimates, it must be corrected in cases of additional water supply, i.e. in irrigation conditions. The correction, which is fully presented and tested in Maselli et al. (2020b), is based on the identification of divergences in the temporal evolutions of meteorological water stress and NDVI, i.e. of cases in which NDVI is increasing or close to the seasonal maximum during intense water stress periods. This concept was introduced by Ozdogan and Gutman (2008), who showed that the combination of meteorological water stress indicators and NDVI data is particularly effective for identifying irrigated croplands in regions characterized by clear summer water limitation. In this environmental situation, long lasting meteorological water stress usually progresses into persistent soil water shortage for rainfed ecosystems (West et al., 2019), while this is obviously not the case if irrigation is applied. The two cases are manifested into diverging green biomass and NDVI evolutions, i.e. decreasing or increasing trends, which provides the basis for the possible deactivation of the meteorological water stress scalar (Maselli et al., 2020b).

The deactivation of the water stress scalar in irrigated conditions permits not only the correct prediction of crop Ta, but also the repartition of this quantity into water supplied by rainfall and by irrigation. While, in fact, the original meteorological scalar is representative of the rain water stored in the soil and usable for transpiration, the modified scalar represents this quantity supplemented by IW. Thus, the two scalars can be used to reduce the estimated Ta for the contribution of rain water stored in the soil. More precisely, IW is obtained from Ta considering both the immediate and the medium-term effects of rainfall. The former simply leads to a three-day irrigation block, while the latter is accounted for through a normalized difference of the modified and original water stress scalars.

The application of this method requires ground and satellite data which are affected by relevant uncertainty. The meteorological data, in particular, are currently derived from a regional database which contains daily estimates of temperature, rainfall and solar radiation with 250 m spatial resolution. The accuracy of these estimates is dependent

on both the number of ground stations utilized and the efficiency of the interpolation algorithm applied (spatially weighted regression, see Thornton et al., 1997; Maselli, 2002). An analysis of both these factors is provided in Chiesi et al. (2007).

The NDVI data are obtained from the processing of S-2 MSI imagery, which contemporaneously offers high spatial resolution (10 m), frequent revisiting time (every 3–4 days) and a standard preprocessed format (Drusch et al., 2012). This allows the production of MVC images which are only marginally affected by atmospheric disturbances and have been further improved by a multitemporal filtering operation (Maselli et al., 2014). In general, the current study confirms the high quality of the radiometrically and atmospherically corrected S-2 MSI L2A product, which, however, implies an NDVI overestimation during periods with low solar irradiation, i.e. from November to February. As already noted by Maselli et al., (2020a), this issue has marginal impact on the current IW estimation method, which is almost completely based on NDVI data taken in spring and summer.

Greater impact is expected from the temporal resolution of the used NDVI MVC images. The 15-day MVC and temporal filtering operations currently applied, in fact, inevitably introduce an approximation in the NDVI estimates, which can be particularly relevant in cases of abrupt green biomass changes, such as those caused by crop harvesting. In these cases the time filters applied can induce an overestimation of the crop greenness, especially when harvesting is performed close to the beginning of each 15-day MVC period. This was actually experimented for the corn field in 2019, when the NDVI drop due to crop harvesting on 19th of August was detected with a 10–15 day delay, causing an overestimation of crop Ta and IW in the last part of the growing cycle.

The conversion of NDVI into FVC is another critical issue which has been currently addressed by applying a generalized linear equation whose local validity has been ascertained in Maselli et al. (2020a). Similar estimates could be obtained from the Sentinel Application Platform (SNAP) biophysical processor, which simulates FVC through the application of an artificial neural network to multispectral S-2 MSI observations (Vuolo et al., 2016; Weiss and Baret, 2016). While, however, the general validity of this approach has been assessed by Wang et al. (2018), its local accuracy should be evaluated by a specific validation effort based on ground observations.

The current method also assumes a unique maximum Kc for all herbaceous species (1.2), which implies that FVC accounts for the entire Kc variability of all annual crops, independently of the type. This is in accordance with previous studies of our research group, which found that such an assumption brings only to a minor approximation in the estimation of ETa for both semi-natural and agricultural herbaceous vegetation types (Maselli et al., 2014, 2020a; Pieri et al., 2019).

The proposed IW estimation method has been tested in various ways during two study years, obtaining generally good results. While nearly null IW is predicted for rainfed winter and spring crops, accurate or reasonable seasonal patterns of IW are predicted for all irrigated summer crops examined. In particular, the estimated IW reproduces both the intensity and timing of the irrigation measured in two experimental fields grown with tomato in 2018 and corn in 2019. The same good estimation capacity is demonstrated for several other fields grown with known annual crops during the two years. In this last case, the estimated IW is in agreement with both the previous experimental observations and the information available about local agricultural practices.

Similarly to previous methods, the current procedure can be adapted for mapping irrigated areas by simply thresholding the estimated IW images. This is not, however, the most efficient utilization of the method, since it implies a notable loss of information in all cases where irrigation is supplemental or limited to specific growing phases. In the study area, for example, some spring crops which are harvested at the beginning of summer (vegetables, chickpea, etc.) are irrigated only occasionally at the end of their growing cycle depending on seasonal meteorology. In these cases, irrigation is partial and limited in time, which explains the low IW estimates found for several fields. While these situations could be addressed by the use of multiple thresholds, the conservation of all information produced on IW is clearly the most preferable option.

The low IW values found for some fields in the study area could be obviously ascribed also to the inherent uncertainty of the method, i.e. to cases when crop NDVI tends to increase during the dry season also in absence of irrigation. These cases could be theoretically due to the presence of alternative water sources which increase soil water availability during the dry season. As can be easily understood, such cases are relatively rare in areas grown with annual crops, where irrigation is usually the prevalent, if not exclusive, water source supplemental to rainfall. An exception to this rule can be represented by areas adjacent to canals, rivers, lakes, swamps, etc., where the presence of a shallow water table can guarantee vigorous plant growth also during prolonged dry periods. In general, however, the geographical position of these areas is stable and known, which allows a simple identification and characterization of such cases.

7. Conclusions

Numerous studies have been conducted in the last decades on the use of remote sensing and ancillary data for identifying and quantifying irrigation patterns (Ozdogan and Gutman, 2008; Ozdogan et al., 2010; Chen et al., 2018; Vogels et al., 2019; Zaussinger et al., 2019). Most of these investigations concern parametric and nonparametric statistical methods, which require complex and tedious training phases and may suffer from poor generalization capacity. Moreover, only most recent works can fully exploit the enhanced spatio-temporal properties of S-2 MSI data, whilst previous studies were mandatorily working at lower spatial resolutions (Chen et al., 2018).

The current research effort is therefore original for both the basic theory and the spatial and temporal scales of investigation. The IW estimation method proposed is, in fact, based on a water balance strategy which was investigated in previous studies and does not require a specific training phase. This method can provide daily IW estimates also in areas characterized by high land cover fragmentation and is generally robust against negative and positive errors, i.e. is capable of identifying both not irrigated and irrigated cropped fields, as well as of predicting the intensity and timing of irrigation events.

From a theoretical point of view, the method relies on the identification of divergent evolutions in meteorological water stress and NDVI, which are obviously more marked in regions where a clear dry season occurs, as is typical of the Mediterranean climate. Consequently, the performance of the method is expected to partly degrade in other, more humid eco-climatic conditions, where the dry season is not so well defined. These situations, in fact, increase the difficulty in distinguishing the NDVI evolutions of rainfed and irrigated crops, creating a general challenge for all methods that identify and characterize irrigated areas (Ozdogan and Gutman, 2008).

It can therefore be concluded that the IW prediction method currently proposed is capable of providing detailed and accurate information on the spatial and temporal distributions of crop irrigation, at least in the examined environmental and agricultural realities. This information can be utilized by public or private environmental stakeholders for planning and regulating the correct uses of water resources, whose demand is notably increasing due to both the ongoing climate change and the rising consume for human activities.

Author statement

F. Maselli: Conceptualization, supervision and writing.
P. Battista: Ground data collection and analysis.
M. Chiesi: Data analysis, writing – review & editing.
B. Rapi: Ground data collection and analysis.
L. Angeli: Ground data collection and processing.

L. Fibbi: Software and data processing.
R. Magno: Data analysis and validation.
B. Gozzini: Supervision and funding acquisition.

Declaration of Competing Interest

The authors report no declarations of interest.

Acknowledgments

The authors wish to thank the farmers who supported the data collection in the experimental and controlled fields, Silvano Dragoni and Uliva Guicciardini. Maurizio Romani, Francesco Sabatini and Alessandro Materassi are thanked for their assistance in the field data collection. Two anonymous JAG reviewers are thanked for their helpful comments on the first draft of the manuscript.

References

Allen, R.G., Pereira, L.S., Raes, D., Smith, M., 1998. Crop Evapotranspiration - Guidelines for Computing Crop Water Requirements - FAO Irrigation and Drainage Paper 56. FAO - Food and Agriculture Organization of the United Nations, Rome.

Ambika, A.K., Brian Wardlow, B., Mishra, V., 2016. Remotely sensed high resolution irrigated area mapping in India for 2000 to 2015. Sci. Data 3, 160118. https://doi.org/10.1038/sdata.2016.118.

Belgiu, M., Csillik, O., 2018. Sentinel-2 cropland mapping using pixel-based and object-based time-weighted dynamic time warping analysis. Remote Sens. Environ. 204, 509–523.

Calera, A., Campos, I., Osann, A., D'Urso, G., Menenti, M., 2017. Remote sensing for crop water management: from ET modelling to services for the end users. Sensors 17, 1104. https://doi.org/10.3390/s17051104.

Chen, Y., Lu, D., Luo, L., Pokhrel, Y., Deb, K., Huang, J., Ran, Y., 2018. Detecting irrigation extent, frequency, and timing in a heterogeneous arid agricultural region using MODIS time series, Landsat imagery, and ancillary data. Remote Sens. Environ. 204, 197–211.

Chiesi, M., Maselli, F., Moriondo, M., Fibbi, L., Bindi, M., Running, S., 2007. Application of BIOME-BGC to simulate Mediterranean forest processes. Ecol. Modell. 206, 179–190.

Drusch, M., Del Bello, U., Carlier, S., Colin, O., Fernandez, V., Gascon, F., Hoersch, B., Isola, C., Laberinti, P., Martimort, P., Meygret, A., Spoto, F., Sy, O., Marchese, F., Bargellini, P., 2012. Sentinel-2: ESA's optical high-resolution mission for GMES operational services. Remote Sens. Environ. 120, 25–36.

Famiglietti, J.S., Rodell, M., 2013. Water in the balance. Science 340 (6138), 1300–1301.

Giannini, A., Bagnoni, V., 2000. Schede di tecnica irrigua per l'agricoltura toscana. ARSIA – Servizio Telematico Irrigazione. Regione Toscana, EFFEMME Lito, Firenze, pp. 66–97 ISBN 88-8295-015-018.

Giorgi, F., Bi, X., Pal, J., 2004. Mean, interannual variability and trends in a regional climate change experiment over Europe. II: climate change scenarios (2071–2100). Clim. Dyn. 23, 839–858. https://doi.org/10.1007/s00382-004-0467-0.

Glenn, E.P., Huete, A.R., Nagler, P.L., Hirschboeck, K.K., Brown, P., 2007. Integrating remote sensing and ground methods to estimate evapotranspiration. Crit. Rev. Plant Sci. 26, 139–168.

Glenn, E.P., Nagler, P.L., Huete, A.R., 2010. Vegetation index methods for estimating evapotranspiration by remote sensing. Surv. Geophys. 31, 531–555.

Gonzalez-Dugo, M.P., Neale, C.M.U., Mateos, L., Kustas, W.P., Prueger, J.H., Anderson, M.C., Li, F., 2009. A comparison of operational remote sensing-based models for estimating crop evapotranspiration. Agric. For. Meteorol. 149, 1843–1853.

Gutman, G., Ignatov, A., 1998. The derivation of the green vegetation fraction from NOAA/AVHRR data for use in numerical weather prediction models. Int. J. Remote Sens. 19, 1533–1543.

Guzinski, R., Nieto, H., 2019. Evaluating the feasibility of using Sentinel-2 and Sentinel-3 satellites for high-resolution evapotranspiration estimations. Remote Sens. Environ. 221, 157–172.

Hartmann, D.L., Tank, A.M.K., Rusticucci, M., Alexander, L.V., Brönnimann, S., Charabi, Y.A.R., Dentener, F.J., Dlugokencky, E.J., Easterling, D.R., Kaplan, A., et al., 2013. Observations: atmosphere and surface. Climate Change 2013 the Physical Science Basis: Working Group I Contribution to the Fifth Assessment Report of the Intergovernmental Panel on Climate Change. Cambridge University Press, Cambridge, UK.

He, M., Kimball, J.S., Yi, Y., Running, S.W., Guan, K., Moreno, A., Wu, X., Maneta, M., 2019. Satellite data-driven modeling of field scale evapotranspiration in croplands using the M.OD16 algorithm framework. Remote Sens. Environ. 230, 111201.

Jalilvand, E., Tajrishy, M., Ghazi Zadeh Hashemi, S.A., Brocca, L., 2019. Quantification of irrigation water using remote sensing of soil moisture in a semi-arid region. Remote Sens. Environ. 231, 111226.

Jensen, M.E., Heise, H.R., 1963. Estimating evapotranspiration from solar radiation. J. Irrig. Drainage Division ASCE 89, 15–41.

Mair, A., Fares, A., 2011. Comparison of rainfall interpolation methods in a mountainous region of a tropical island. J. Hydrol. Eng. 16 (4), 371–383.

Maselli, F., 2002. Improved estimation of environmental parameters through locally calibrated multivariate regression analyses. Photogramm. Eng. Remote Sens. 68 (11), 1163–1171.

Maselli, F., Papale, D., Chiesi, M., Matteucci, G., Angeli, L., Raschi, A., Seufert, G., 2014. Operational monitoring of daily evapotranspiration by the combination of MODIS NDVI and ground meteorological data: application and validation in Central Italy. Remote Sens. Environ. 152, 279–290.

Maselli, F., Angeli, L., Battista, P., Fibbi, L., Gardin, L., Magno, R., Rapi, B., Chiesi, M., 2020a. Evaluation of MODIS and MSI NDVI data for predicting actual evapotranspiration in Mediterranean areas. Int. J. Remote Sens. 41 (14), 5186–5205.

Maselli, F., Angeli, L., Chiesi, M., Fibbi, L., Rapi, B., Romani, M., Sabatini, F., Battista, P., 2020b. An improved NDVI-based method to predict actual evapotranspiration of irrigated grasses and crops. Agric. Water Manag. 233. https://doi.org/10.1016/j.agwat.2020.106077.

Mu, Q., Zhao, M., Running, S.W., 2011. Improvements to a MODIS global terrestrial evapotranspiration algorithm. Remote Sens. Environ. 115, 1781–1800.

Ozdogan, M., Gutman, G., 2008. A new methodology to map irrigated areas using multi-temporal MODIS and ancillary data: an application example in the continental US. Remote Sens. Environ. 112, 3520–3537.

Ozdogan, M., Yang, Y., Allez, G., Cervantes, C., 2010. Remote sensing of irrigated agriculture: opportunities and challenges. Remote Sens. 2 (9), 2274–2304.

Peña-Arancibia, J.L., McVicar, T.R., Paydar, Z., Li, L., Guerschman, J.P., Donohue, R.J., Dutta, D., Podger, G.M., van Dijk, A.I.J.M., Chiew, F.H.S., 2014. Dynamic identification of summer cropping irrigated areas in a large basin experiencing extreme climatic variability. Remote Sens. Environ. 154, 139–152.

Pereira, L.S., Allen, R.G., Smith, M., Raes, D., 2015. Crop evapotranspiration estimation with FAO56: past and future. Agric. Water Manag. 147, 4–20.

Pieri, M., Chiesi, M., Battista, P., Fibbi, L., Gardin, L., Rapi, B., Romani, M., Sabatini, F., Angeli, L., Cantini, C., Giovannelli, A., Maselli, F., 2019. Estimation of actual evapotranspiration in fragmented Mediterranean areas by the spatio-temporal fusion of NDVI data. IEEE J. Sel. Top. Appl. Earth Obs. Remote. Sens. 12, 5018–51017.

Senay, G.B., 2008. Modeling landscape evapotranspiration by integrating land surface phenology and a water balance algorithm. Algorithms 1, 52–68.

Steduto, P., Hsiao, T.C., Fereres, E., Raes, D., 2012. Crop Yield Response to Water. – FAO Irrigation and Drainage Paper 66. FAO - Food and Agriculture Organization of the United Nations, Rome ISBN 978-92-5-107274-107275.

Thornton, P.E., Running, S.W., White, M.A., 1997. Generating surfaces of daily meteorological variables over large regions of complex terrain. J. Hydrol. 190, 214–251.

Thornton, P.E., Hasenauer, H., White, M.A., 2000. Simultaneous estimation of daily solar radiation and humidity from observed temperature and precipitation: an application over complex terrain in Austria. Agric. For. Meteorol. 104, 255–271.

Vanino, S., Nino, P., De Michele, C., Falanga Bolognesi, S., D'Urso, G., Di Bene, C., Pennelli, B., Vuolo, F., Farina, R., Pulighe, G., Napoli, R., 2018. Capability of Sentinel-2 data for estimating maximum evapotranspiration and irrigation requirements for tomato crop in Central Italy. Remote Sens. Environ. 15, 452–470.

Vogels, M.F.A., de Jong, S.M., Sterk, G., Addink, E.A., 2019. Mapping irrigated agriculture in complex landscapes using SPOT6 imagery and object-based image analysis – a case study in the Central Rift Valley, Ethiopia. Int. J. Appl. Earth Obs. Geoinf. 75, 118–129.

Vuolo, F., Zółtak, M., Pipitone, C., Zappa, L., Wenng, H., Immitzer, M., Weiss, M., Baret, F., Atzberger, C., 2016. Data service platform for Sentinel-2 surface reflectance and value-added products: system use and examples. Remote Sens. 8, 938. https://doi.org/10.3390/rs8110938.

Wang, B., Jia, K., Liang, S., Xie, X., Wei, X., Zhao, X., Yao, Y., Zhang, X., 2018. Assessment of Sentinel-2 MSI spectral band reflectances for estimating fractional vegetation cover. Remote Sens. 10, 1927. https://doi.org/10.3390/rs10121927.

Weiss, M., Baret, F., 2016. S2 ToolBox Level 2 Products: LAI, FAPAR, FCOVER Version 1.1. Available from:. http://step.esa.int/docs/extra/ATBD_S2ToolBox_L2B_V1.1.pdf.

West, H., Quinn, N., Horswell, M., 2019. Remote sensing for drought monitoring & impact assessment: progress, past challenges and future opportunities. Remote Sens. Environ. 232, 111251. https://doi.org/10.1016/j.rse.2019.111291.

Zaussinger, F., Dorigo, W., Gruber, A., Tarpanelli, A., Filippucci, P., Brocca, L., 2019. Estimating irrigation water use over the contiguous United States by combining satellite and reanalysis soil moisture data. Hydrol. Earth Syst. Sci. 23, 897–923.

Zhang, K., Kimball, J.S., Running, S.W., 2016. A review of remote sensing based actual evapotranspiration estimation. WIREs Water 3, 834–853. https://doi.org/10.1002/wat2.1168.